Proceedings of the 2010 ASME International Manufacturing Science and Engineering Conference
MSEC2010
October 12-15, 2010, Erie, Pennsylvania, USA

MSEC2010-34234

MICROSTRUCTURAL CHANGES OF AZ31 MAGNESIUM ALLOYS INDUCED BY CRYOGENIC MACHINING AND ITS INFLUENCE ON CORROSION RESISTANCE IN SIMULATED BODY FLUID FOR BIOMEDICAL APPLICATIONS

Z. Pu, O. W. Dillon, Jr. and I. S. Jawahir
University of Kentucky
Department of Mechanical Engineering, and
Institute for Sustainable Manufacturing
Lexington, Kentucky, USA

D. A. Puleo
University of Kentucky
Center for Biomedical Engineering
Wenner-Gren Lab
Lexington, Kentucky, USA

ABSTRACT

Poor corrosion resistance is one of the major disadvantages of magnesium alloys that inhibits their wide application. It was reported frequently that the alloys' microstructure has a significant influence on their corrosion resistance. In this study, cryogenic machining is used as a severe plastic deformation tool to modify the surface and subsurface microstructures of an AZ31 Mg alloy. Liquid nitrogen is applied to suppress grain growth caused by large heat generation during machining. "White layers", where grain boundaries were invisible, were shown to form on the surface and subsurface after machining. The hardness of this layer was about 60% larger than the bulk material. The tool edge radius and the cutting speed have profound influence on the microstructures. Preliminary results from immersion tests in simulated body fluid showed that the corrosion resistance of the AZ31 Mg alloy was enhanced due to the formation of white layer.

INTRODUCTION

Magnesium alloys have been considered as a promising lightweight structural material for both automotive and aerospace applications for a long time. Recently, new application of magnesium alloys as a novel biodegradable material for temporary internal fixation implants is also emerging [1]. However, one major limitation of the wide application is their unsatisfactory corrosion performance.

Although various approaches, such as alloying and coating, have been explored extensively by researchers, the potential of grain refinement on improved corrosion resistance has not been fully investigated. Hot rolled AZ31 Mg alloy samples were reported to have a marked reduction in corrosion rate compared with squeeze cast samples, which was attributed to grain refinement from 450 μm to 20 μm [2]. However, further grain refinement by equal channel angular pressing (ECAP) to 2.5 μm did not decrease the corrosion rate. With the same material, Alvarez-Lopez et al. [3] found that samples with 4.5 μm grain size processed by ECAP and followed by rolling had better corrosion resistance than the initial samples with 25.7 μm grains. Aung and Zhou [4] also reported that an increase from 65 μm to 250 μm led to a significant increase in corrosion rates.

To achieve grain refinement in magnesium alloys, severe plastic deformation (SPD) processes, such as ECAP and high pressure torsion (HPT), are widely used. However, the lowest possible grain sizes reported by most of the researchers are larger than or close to 1 μm. This limitation is attributed to the small strain-rate ($<10^2$ s^{-1}) and the heating that is normally needed to facilitate the processing. Machining is a SPD process where strain and strain-rate are controllable through changing cutting parameters. The strain-rate achievable by machining can be as large as 10^5 s^{-1} [5]. Significant grain refinement has been reported on the machined surface layers. Nanocrystallized grains of about 5-20 nm were reported on the top of the white layer of AISI 52100 steel after machining [6]. Ultrafine grains about 175 nm were shown to form on the machined surface of copper [7].

However, due to grain growth caused by the large amount of heat generated during machining, these nanocrystallized grains can be found only at the top surface of the machined component, and the cutting speed is limited to a very low range. Also, only a few studies report the use of machining as a SPD tool to introduce grain refinement in magnesium alloys.

In the present study, liquid nitrogen is used to reduce the temperature rise during machining. The effects of cutting conditions on microstructural changes of the AZ31 Mg alloy are investigated. The influence of machining on corrosion resistance is also studied using an *in vitro* corrosion setup.

EXPERIMENTAL WORK

Work Material

The work material studied was the commercial AZ31 B-O magnesium alloy. It was obtained in the form of a 3 mm thick sheet. Disc specimens were made from the sheet (3 mm in thickness and 130 mm in diameter) and subsequently subjected to orthogonal machining. It is noted that turning is used as the final step to prepare the discs from the sheet in the machine shop.

Machining Experiments

A Mazak Quick Turn-10 Turning Center equipped with an Air Products liquid nitrogen delivery system is used to conduct orthogonal turning on the AZ31 Mg discs. As shown in Figure 1, liquid nitrogen was sprayed at the machined surface from the clearance side of the cutting tool for cryogenic machining.

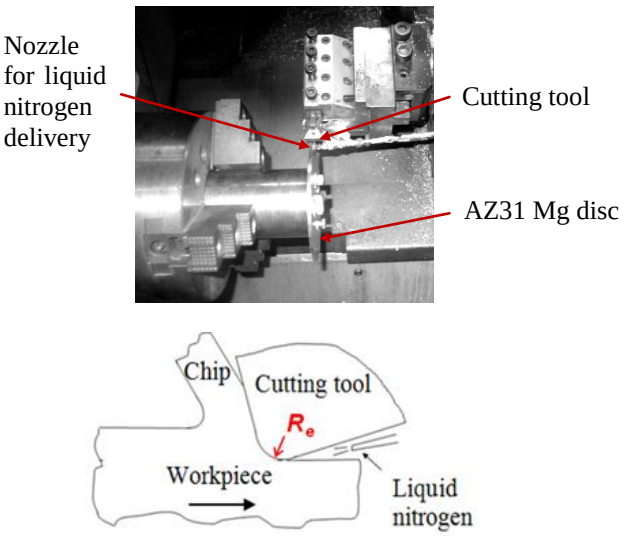

FIGURE 1 - MACHINING SETUP WITH A LIQUID NITROGEN DELIVERY SYSTEM

The cutting tool used was uncoated carbide C5/C6 inserts from Kennametal. The edge radius of the cutting tools (R_e) was prepared by grinding to two different values. The actual tool edge radius before machining was measured using a ZYGO New View 5300 measurement system.

Two sets of machining experiments were conducted. The experiment matrix is shown in Table 1. For the first set, the cooling method and tool edge radius were changed to investigate their influence on microstructural changes. For the second set, the tool edge radius and the feed rate were fixed and only the cutting speed was varied.

TABLE 1 - MATRIX FOR THE MACHINING EXPERIMENTS

SET 1 – Cooling Method and Tool Edge Radius

No.	Cooling Method	Tool Edge Radius (µm)	Cutting Speed (m/min)	Feed Rate (mm/rev)
1	Dry	30	100	0.1
2	Cryogenic	30	100	0.1
3	Cryogenic	68	100	0.1

SET 2 – Cutting Speed

No.	Cooling Method	Tool Edge Radius (µm)	Cutting Speed (m/min)	Feed Rate (mm/rev)
4	Cryogenic	70	50	0.15
5	Cryogenic	70	100	0.15
6	Cryogenic	71	150	0.15

Characterization Methods

Metallurgical samples were cut from the machined discs. After cold mounting, grinding and polishing, acetic picric solution was used as the etchant to reveal the grain structure. Optical microscope and scanning electron microscopes (SEM) were used to observe the microstructure of the AZ31 Mg discs.

Microindentation tests were performed using a Vickers indenter on a CSM Micro-Combi Tester. The load used was 50 mN and the duration time was 10s.

In vitro Corrosion Test

The corrosion resistance of machined AZ31 Mg discs was examined in simulated body fluid (SBF) with a composition: 8.0 g/l NaCl, 0.4 g/l KCl, 0.14 g/l $CaCl_2$, 0.35 g/l $NaHCO_3$, 1.0 g/l D-glucose, 0.2 g/l $MgSO_4 \cdot 7H_2O$, 0.1 g/l $KH_2PO_4 \cdot H_2O$ and 0.06 g/l $Na_2HPO_4 \cdot 7H_2O$. The *pH* value of the SBF was adjusted to 7.4. The solution was kept in an incubator to maintain the temperature at 37 ± 1 ℃. To evaluate the biodegradation rates, hydrogen evolution method [8] was used to continually monitor the corrosion process for 15 days. To reduce the effects of *pH* increase and accumulation of corrosion products on corrosion rate, large solution volume/surface area (SV/SA) ratio (SV/SA=433) was used [9]. The corrosion setup is shown in Figure 2.

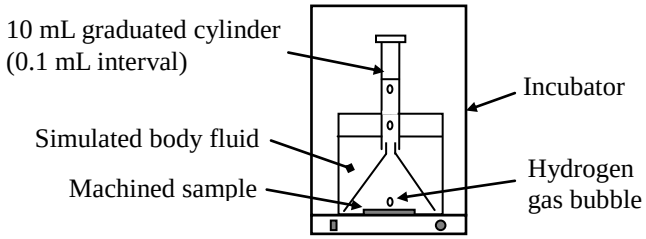

FIGURE 2 - IN VITRO CORROSION SETUP

RESULTS AND DISCUSSION

The initial microstructure of the AZ31 Mg disc is shown in Figure 3. There is no twinning in the bulk material since the as-received material is a fully annealed sheet. However, twinning is visible near the surface of the disc, which is due to the sample preparation in the machine shop where a turning operation is used as the final step in making the disc.

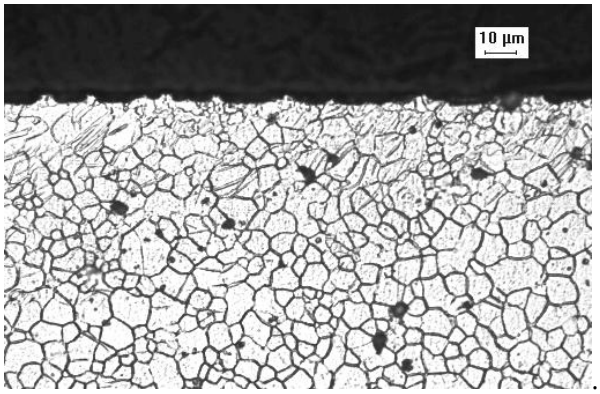

FIGURE 3 - INITIAL MICROSTRUCTURE OF THE AZ31 MAGNESIUM DISC BEFORE MACHINING EXPERIMENTS

SET 1 – Cooling Method and Tool Edge Radius

Figure 4 shows the microstructures obtained under conditions from Set 1 of the experiment matrix (Table 1). Significant changes on microstructures near the machined surface were found. The grain boundaries were clearly visible under dry machining using a tool with 30 µm edge radius (Figure 4(A)). However, a surface layer of about 8 µm in which grain boundaries were no longer visible at this magnification formed when liquid nitrogen was applied (Figure 4(B)). This layer increased to about 15 µm when the edge radius of the tool was changed to 68 µm (Figure 4(C)). This layer of indiscernible grain structure was also reported in other materials after machining, especially in hardened steels, where the term "white layer" was frequently used [6]. Nanocrystallized grains of about 5-20 nm in size were found in this layer. The layer formed here is also similar to the layer reported by Li et al. [10] on pure copper prepared by another SPD process where liquid nitrogen was also applied. The grain size on the top of that layer was 20 nm measured by TEM.

Smaller grain size leads to larger hardness values according to the Hall-Petch relationship established experimentally in AZ31 Mg alloys [11]. The hardness profiles of the disc before the machining experiments (initial), after dry machining with a 30 µm tool and cryogenic machining with a 68 µm tool are shown in Figure 5. Those samples were selected because they had a large contrast in terms of microstructure.

The initial hardness of the material is 60 HV. The hardness values near to the surface on these three profiles were increased to different extents. The increase of hardness in the initial disc is due to the disc preparation in the machine shop. This conclusion is supported by the twinning observed in Figure 3. The increase of hardness in the dry machined disc using a 30 µm tool is similar to the increase of the initial disc. The similarity is expected since the machine shop also uses dry machining for the preparation of the discs. The increase in the disc after cryogenic machining, however, is the largest. The hardness at about 5 µm from the surface was increased about 60% compared with the bulk material. It is noted that the hardness values near the surface are normally underestimated due to edge softening effects. Therefore, the actual hardness increase should be even larger than 60%. This large increase in

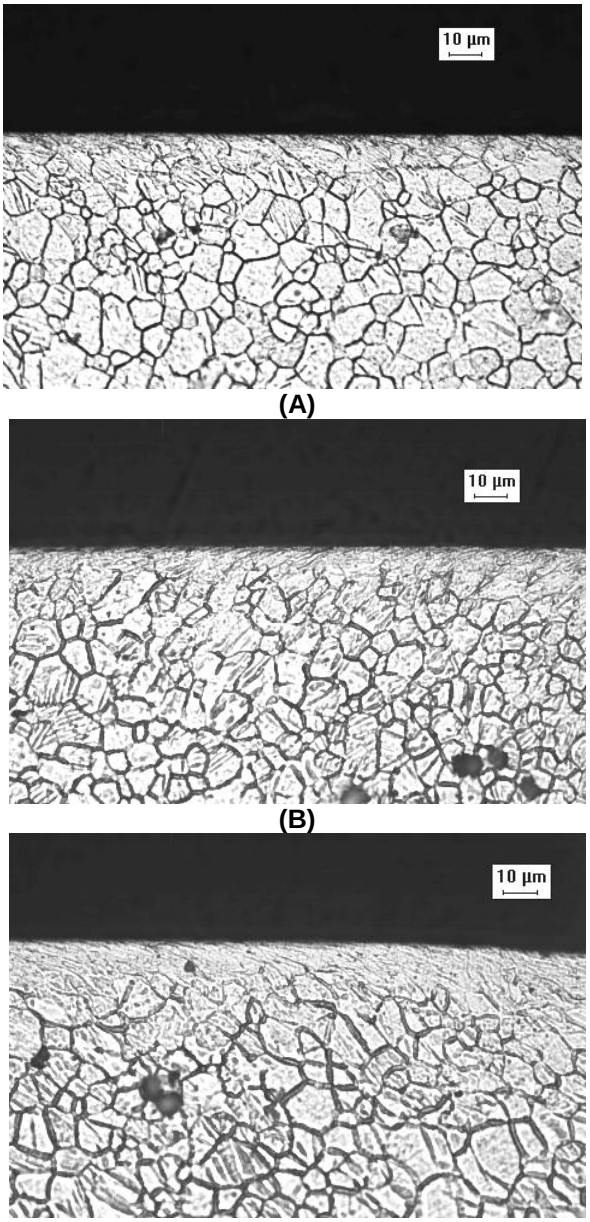

FIGURE 4 - MICROSTRUCTURE OF AZ31 MAGNESIUM DISCS AFTER MACHINING: (A) DRY MACHINING, TOOL EDGE RADIUS = 30 µm, (B) CRYOGENIC MACHINING, TOOL EDGE RADIUS = 30 µm, (C) CRYOGENIC MACHINING, TOOL EDGE RADIUS = 68 µm.

hardness suggests that the white layer formed on cryogenic machined AZ31 Mg disc may have similar nanocrystallized grains as those found in SPD-processed copper and steels, which make it very difficult for optical microscopy techniques to accurately capture the grain boundaries.

An empirical formula established by Watanabe et al. [12] in Mg AZ 31 was used by Chang [13] to predict the size of the recrystallized grains after friction stir process (FSP) with the application of liquid nitrogen and the prediction was reported to be consistent with the experimental results in the AZ31 Mg alloy. The formula is:

$$\frac{d_{rec}}{d_{init}} = 10^3 \times Z^{-1/3} = 10^3 \times [\dot{\varepsilon} \times \exp(\frac{Q}{RT})]^{-1/3} \quad (1)$$

where d_{rec} is the recrystallized grain size, d_{init} is the initial grain size, Z is the Zener-Hollomon parameter, $\dot{\varepsilon}$ is the strain-rate, Q is the activation energy, R is the gas constant and T is the temperature. The upper bound of the recrystallized grains after cryogenic machining can be estimated using this formula. The upper bound of initial grain size d_{init} is 10 µm. Reasonable assumptions on the temperature and the strain-rate can be made respectively based on the results from finite element modeling (FEM) of the machining process reported by Salahshoor et al. [14] and Ceretti et al. [15]. The maximum temperature is assumed to be 250 ℃. The minimum strain-rate is assumed to be 10^3 s^{-1}. These values will lead to the upper bound of the recrystallized grain size based on Equation 1. The predicted grain size value is 32 nm. Compared with the 250 nm achieved by friction stir processing [13], this significant decrease in grain size was mainly due to the large increase in strain-rate from 36 s^{-1} to 10^3 s^{-1}. The predicted value explains the large increase in hardness after cryogenic machining. TEM analysis will be conducted in the future to verify this prediction.

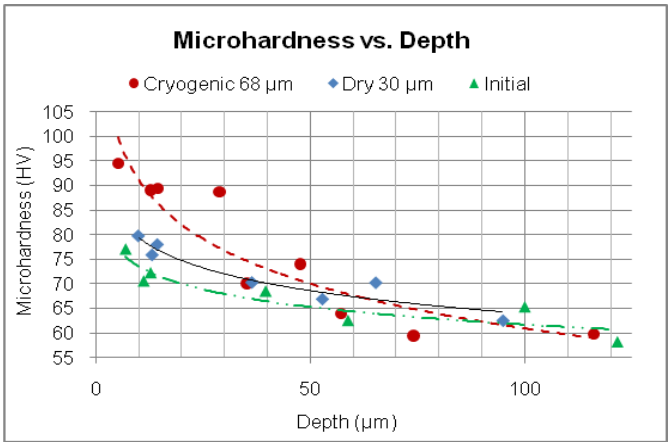

FIGURE 5 – HARDNESS PROFILE OF AZ31 MAGNESIUM DISCS UNDER DIFFERENT MACHINING CONDITIONS

SET 2 – Cutting Speed

The strain-rate during machining is directly proportional to the cutting speed. To investigate the influence of cutting speed on the microstructure of AZ31 Mg discs, three different speeds were selected ranging from 50 m/min to 150 m/min. The cooling conditions are all cryogenic; the tool edge radius is kept the same at 70 µm; the feed rate is 0.15 mm/rev. The microstructures under different cutting speed are shown in Figure 6.

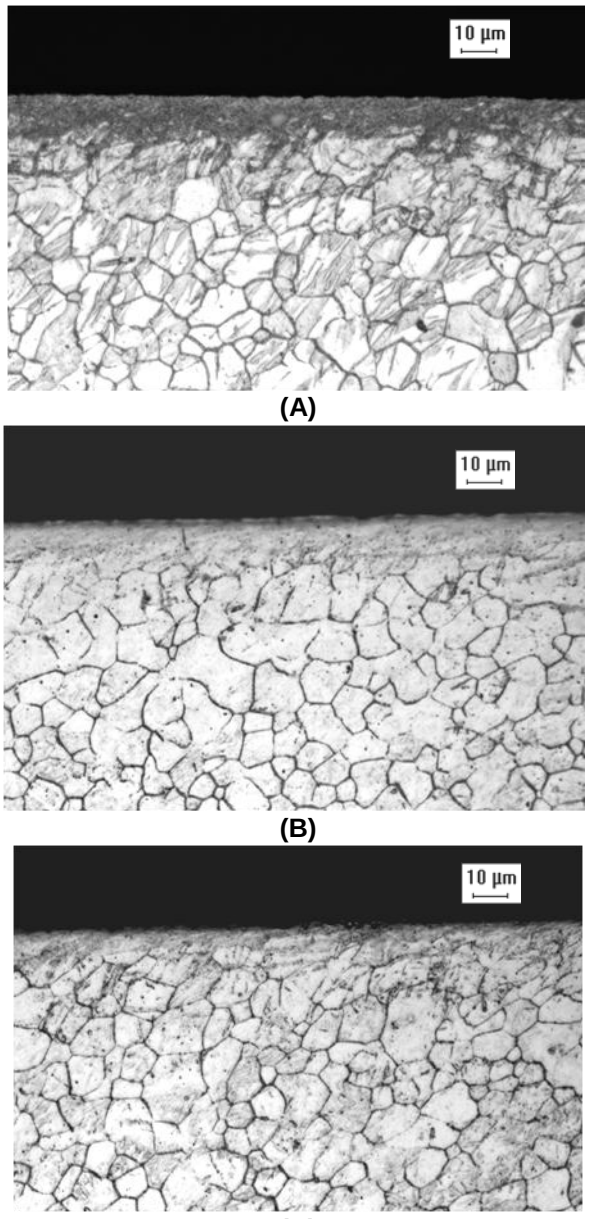

FIGURE 6 - MICROSTRUCTURE OF AZ31 MAGNESIUM DISCS AFTER CRYOGENIC MACHINING: (A) CUTTING SPEED = 50 m/min, (B) CUTTING SPEED = 100 m/min, (C) CUTTING SPEED = 150 m/min.

Remarkable differences, compared with the initial microstructure shown in Figure 3, occur near the machined surface of the AZ31 Mg discs. The influence of cutting speed on microstructural changes is significant. The top layer under 50 m/min has a darker appearance while the one under 100

m/min is similar to the white layer shown in Figure 4(C). This similarity is caused by the similarity in cutting conditions. All the other conditions are the same except that the feed rate is increased from 0.1 mm/rev to 0.15 mm/rev for disc No. 4. Noteworthy differences in the microstructures below the top layers are also evident. While there is no twinning visible under 100 m/min (Figure 6(A)), it is visible up to more than 50 μm away from the top surface under 50 m/min (Figure 6(B)). The microstructure under 150 m/min is different from both 50 m/min and 100 m/min. It does not have an apparent layer near the surface and no twinning is visible (Figure 6(C)).

To explore the possible causes for the differences in microstructures, the chips from the corresponding machining experiment were collected and shown in Figure 7. There are significant changes in the chip morphology under different cutting conditions. The chip shape changed from needle (Figure 7(A)) to short, discontinuous ribbon (Figure 7(B)) when the cutting speed was increased from 50 m/min to 100 m/min. The needle chips indicate that the ductility of the workpiece is relatively low. Given the same work material, this decrease in ductility suggests that the temperature at the cutting zone is relatively lower. It is known that higher cutting speed generally leads to larger temperature rise during machining. Further increase in the cutting speed to 150 m/min changes the chip morphology to long, continuous ribbons, which indicate even better ductility. It is also apparent that the machined surface undergoes similar thermal affects. Therefore, it can be concluded from the chip morphology that there are notable temperature rises when the cutting speed was changed from 50 m/min to 150 m/min and also the ductility of the AZ31 Mg alloy is very sensitive to temperature.

According to the above discussion, it can be stated that the twinning formation at low cutting speed may be due to the low temperature generated at the cutting zone. Kurihara et al. [16] reported that the temperature during dry machining of AZ31 Mg alloys was 150 ℃ at 100 m/min cutting speed, 0.32 mm/rev feed rate and 3 mm depth of cut. The disc whose microstructure is shown in Figure 6(A) was machined under similar cutting conditions except that the feed rate was smaller (0.15 mm/rev) and with liquid nitrogen as the coolant. Therefore, it is reasonable to assume that the temperature is below 100 ℃. Due to the low temperature and large severe plastic deformation imposed on the AZ31 Mg disc by machining, it is expected that twinning will be generated near the surface. The radial force may also be higher compared with 100 m/min cutting speed since the temperature is lower when cutting at 50 m/min, which can explain why the effect of machining extends to more depth into the bulk material. When the cutting speed was increased to 100 m/min, the temperature in the cutting zone was higher. This may generate a favorable combination of temperature and strain-rate that facilitates dynamic recrystallization (DRX). Therefore, a white layer similar to Figure 4(C) was formed. Further increase in cutting speed to 150 m/min leads to a significant reduction in white layer thickness to about 2 μm. This may be due to the possibility that the large temperature rise caused by increased cutting speed surpasses the benefits

(A)

(B)

(C)

FIGURE 7 – CHIP MORPHOLOGY IN MACHINING AZ31 MAGNESIUM DISCS UNDER: (A) CRYOGENIC MACHINING, CUTTING SPEED = 50 m/min, (B) CRYOGENIC MACHINING, CUTTING SPEED = 100 m/min, (C) CRYOGENIC MACHINING, CUTTING SPEED = 150 m/min.

from increased strain-rate. An infrared thermal imaging system will be used in future experiment to verify this hypothesis

To investigate the possible structure of the surface layer formed on Disc 4 (Figure 6(A)) and how the transition from the bulk material to the surface layer occurs, SEM was used to observe the surface microstructure. Figure 8(A) shows the microstructure of the Mg AZ 31 disc after cryogenic machining using a tool with 70 μm edge radius at 50 m/min. Twinning and grain boundaries are clearly visible about 10 μm away from the surface while there are no apparent grain structures in the top surface layer. An expanded view of that layer is shown in Figure 8(B). Under ×5000 magnification, no discernable structure can be found. A transition occurs in Figure 8(C) which is taken below Figure 8(B). Grain boundaries are clearly visible in the bottom half of the figure while they become vague in the top half. The mechanism of grain refinement in Mg AZ91 alloys was shown to take place in three steps by Sun et al. [17]. Twinning was claimed as the first step of grain refinement. Then dislocation movements on both basal plane and non-basal

plane slip systems lead to dislocation arrays which become the subgrain boundaries with high stored energy. The final step is dynamic recrystallization, which leads to nanocrystallized grains. According to this theory, Figure 8(B) may consist of complex dislocation arrays. On the topmost surface, DRX may occur and nanocrystallized grains may be formed. TEM analysis will be used to provide more information about the possible grain structure and the grain refinement mechanism.

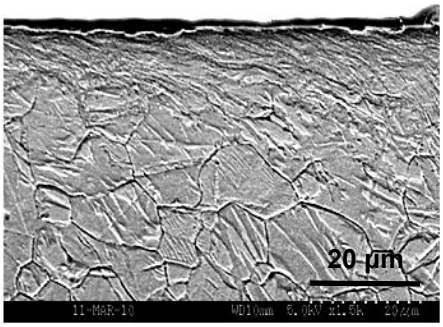

(A)

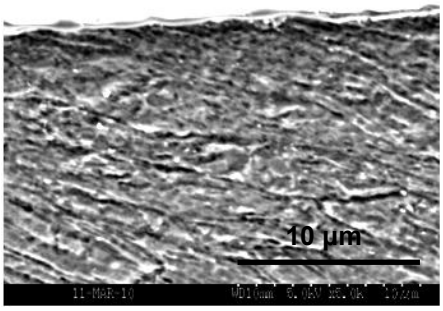

(B)

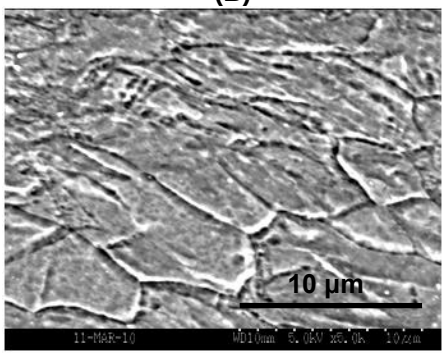

(C)

FIGURE 8 – MICROSTRUCUTRE AFTER CRYOGENIC MACHINING (TOOL EDGE RADIUS = 68 µm) , CUTTING SPEED = 50 m/min: (A) OVERVIEW, X1500 (B) TOP SURFACE LAYER, X5000 (C) BELOW THE TOP LAYER, X5000

Corrosion Test

The influence of the microstructural changes on corrosion resistance in SBF was studied using an *in vitro* corrosion test. The disc under dry machining using a tool with 30 µm edge radius and the one under cryogenic machining using a tool with 68 µm edge radius were selected to undergo the corrosion test due to their large difference in microstructure. The preliminary results of the corrosion test are shown in Figure 9. The corrosion rates of the two discs are close to each other in the first two days. This may be due to formation of a thin passivated layer formed by oxidation during the machining process on both samples. After about two days, the disc from dry machining suffers more corrosion than the one after cryogenic machining. However, after about 7 days, the corrosion rate of this disc started to decrease while the one from cryogenic machining kept its corrosion rate. The total volume of the evaluated hydrogen gas became almost the same after 10 days. This may be caused by the dissolution of the white layer on the cryogenic machined disc. This preliminary result indicates that the white layer formed during cryogenic machining may improve the corrosion resistance in SBF. However, more corrosion tests and other test methods, such as electrochemical and mass loss methods, will be used in the future to confirm these preliminary results.

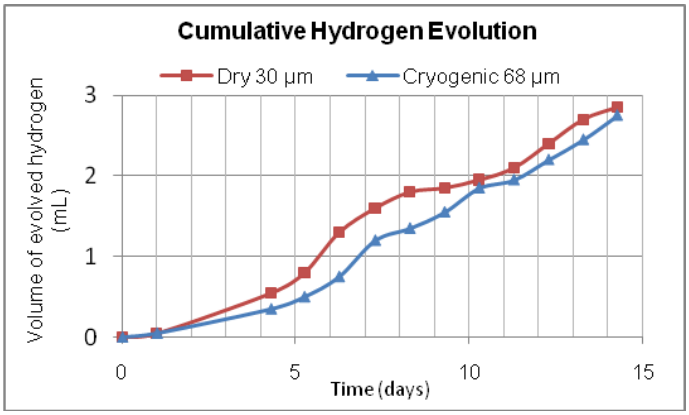

FIGURE 9 – HYDROGEN EVOLUTION DURING IN VITRO CORROSION TEST

CONCLUSION

The microstructure of AZ31 Mg alloys can be significantly altered by changing machining conditions. A white layer where grain structures are not discernable can be produced using cryogenic machining. The hardness of this layer was shown to increase about 60% compared with the bulk material. Nanocrystallized grains may be formed in this layer. Increasing the edge radius of the tool leads to a thicker white layer. Using the same edge radius, the microstructure of AZ31 Mg alloy is very sensitive to cutting speed. The *in vitro* corrosion test shows that the white layer may improve the corrosion resistance of AZ31 Mg alloy in SBF.

The results from the present study reveal the potential for use of machining as a SPD tool for generating a grain refinement layer on surface and subsurface. The critical parameters of a SPD process such as strain and strain-rate can be adjusted relatively easily by changing the cutting conditions. The temperature effects can also be investigated by adjusting cooling method.

Compared with other SPD processes, machining has several major advantages. It is a continuous SPD process with

relatively high processing speed. Machining is widely used in industry, and the application of liquid nitrogen requires little capital investment. Also, the existing empirical and theoretical knowledge on machining will significantly facilitate the development of predictive models to make the SPD process more controllable.

However, systematic studies are needed to further investigate the influence of various machining conditions on microstructural changes of AZ31 Mg alloys. Also, more corrosion tests are needed to establish a clearer relationship between the microstructure and the corrosion resistance.

ACKNOWLEDGMENTS

The equipment for liquid nitrogen application is provided by Air Products and Chemicals. The authors sincerely thank their support for the experimental work. The authors would also like to thank Dr. Fuqian Yang (Department of Material Science, University of Kentucky) for providing the guidance and equipment for microhardness measurement.

REFERENCES

[1] Frank Witte, Norbert Hort, Carla Vogt, Smadar Cohen, Karl Ulrich Kainer, Regine Willumeit and Frank Feyerabend (2008). "Degradable biomaterials based on magnesium corrosion". *Current Opinion in Solid State and Materials Science*, 12, pp. 63-72.

[2] H. Wang, Y. Estrin and Z. Zuberova (2008). "Bio-corrosion of a magnesium alloy with different processing histories". *Materials Letters*, 62, pp. 2476-2479.

[3] M. Alvarez-Lopez, Mar á Dolores Pereda, J.A. del Valle, M. Fernandez-Lorenzo, M.C. Garcia-Alonso, O.A. Ruano and M.L. Escudero (2009). "Corrosion behaviour of AZ31 magnesium alloy with different grain sizes in simulated biological fluids", *Acta Biomaterialia*, Article in Press, Corrected Proof.

[4] Naing Naing Aung and Wei Zhou (2010). "Effect of grain size and twins on corrosion behaviour of AZ31B magnesium alloy ". *Corrosion Science*, 52, pp. 589-594.

[5] Srinivasan Swaminathan, M. Ravi Shankar, Seongyl Lee, Jihong Hwang, Alexander H. King, Renae F. Kezar, Balkrishna C. Rao, Travis L. Brown, Srinivasan Chandrasekar, W. Dale Compton, Kevin P. Trumble (2005). "Large strain deformation and ultra-fine grained materials by machining". *Materials Science and Engineering A*, 410–411, pp. 358–363.

[6] A. Ramesh, S.N. Melkote, L.F. Allard, L. Riester, T.R. Watkins (2005), "Analysis of white layers formed in hard turning of AISI 52100 steel", *Materials Science and Engineering A*, 390, pp.88–97.

[7] R. Calistes, S. Swaminathan, T.G. Murthy, C. Huang, C. Saldana, M.R. Shankar and S. Chandrasekar (2009). "Controlling gradation of surface strains and nanostructuring by large-strain machining". *Scripta Materialia*, 60, pp.17–20.

[8] Song, G., Atrens, A., St John, D. H. (2001). "An hydrogen evolution method for the estimation of the corrosion rate of magnesium alloys". *Proceeding of Magnesium Technology 2001*, TMS Annual Meeting. New Orleans, LA. February 11-15.

[9] Lei Yang, Erlin Zhang (2009). "Biocorrosion behavior of magnesium alloy in different simulated fluids for biomedical application", *Materials Science and Engineering C*, 29, pp.1691–1696.

[10] W.L. Li, N.R. Tao, K. Lu (2008). "Fabrication of a gradient nano-micro-structured surface layer on bulk copper by means of a surface mechanical grinding treatment". *Scripta Materialia*, 59, pp.546–549.

[11] C.I. Chang, C.J. Lee, J.C. Huang (2004). "Relationship between grain size and Zener–Holloman parameter during friction stir processing in AZ31 Mg alloys". *Scripta Materialia*, 51, pp. 509-514.

[12] H. Watanabe, H. Tsutsui, T. Mukai, K. Ishikawa, Y. Okanda, M. Kohzu and K. Higashi (2001). "Grain size control of commercial wrought Mg-Al-Zn alloys utilizing dynamic recrystallization", *Materials Transactions (Japan)*, 42, pp. 1200-1205.

[13] Chih-I Chang (2007). "Achieving Ultrafine Nano Grains in AZ31 Mg Based Alloys and Composites by Friction Stir Processing".PhD thesis, National Sun Yat-sen University, Taiwan, R.O.C.

[14] M. Salahshoor, Y.B. Guo (2009). "Numerical Modeling and Simulation of High Speed Machining Biomedical Magnesium Calcium Alloy". *Proceedings of ASM 2009 Materials & Processes for Medical Devices Conference*, Minneapolis, Minnesota.

[15] E. Ceretti, P. Fallböhmer, W. T. Wu, T. Altan (1996). "Application of 2D FEM to chip formation in orthogonal cutting". *Journal of Materials Processing Technology*, 59, pp.169-180.

[16] K Kurihara, T Tozawa, H Kato (1981). "Cutting Temperature of Magnesium Alloys at Extremely High Cutting Speeds". *Journal of Japan Institute of Light Metals*, 31, pp. 255-260.

[17] H.Q. Sun, Y.-N. Shi, M.-X. Zhang, K. Lu (2007). "Plastic strain-induced grain refinement in the nanometer scale in a Mg alloy", *Acta Materialia*, 55, pp. 975–982.